Optimal Traveling-Wave Fault Locator Deployment and Performance Assessment: A Dominion Energy Case Study

Te-Yu Lin, Keanan A. Zafar, Robert M. Orndorff, Micah J. Till, PhD
Dominion Energy Virginia
Richmond, Virginia

***Abstract*—Over the past decade, Dominion Energy Virginia has successfully deployed traveling-wave fault locators (TWFLs) on its 500 kV system, which have demonstrated excellent results in locating faults. Encouraged by the result, we began to explore the potential to expand traveling-wave fault locator installation across the rest of Dominion Energy's transmission system, which includes substations operating at 230 kV, 138 kV, 115 kV, and 69 kV. However, with more than 400 substations operating at these voltages, location selection is challenging. This paper presents an analytical approach to identifying the minimum number of fault locators required to achieve comprehensive system coverage and how to strategically determine their optimal locations to enhance cost effectiveness. Installation priority is based upon multiple factors including line length, fault history, connected customers, line homogeneity, and the capability of software-based methods to indirectly monitor multiple lines. This process is outlined in detail to provide others with the ability to replicate the study with a different power system. This paper also evaluates various traveling-wave-based products and develops a monitoring strategy to guide Dominion's future hardware selection and installation. A series of test scenarios with frequency-dependent line models were created for hardware-in-the-loop (HIL) simulation and testing using a real-time electromagnetic transient power system simulator.**

Keywords— traveling wave fault locator, optimal deployment, hardware-in-the-loop, real-time electromagnetic transient power system simulator

I. Introduction

The first traveling-wave fault locators (TWFLs) were installed on Dominion Energy Virginia's system in 2008 as part of a pilot program to evaluate the equipment's effectiveness and assess its ability to accurately locate faults compared to a traditional digital fault recorder (DFR). During the pilot [1], TWFLs were installed on lines where we had trouble locating faults, which were all 115 kV lines. The lines did have distinctive characteristics—one was very old construction with poor grounding, and another terminated into the low side of a 500/115 kV transformer. The lines were primarily chosen because they all experienced a higher-than-average number of faults. All TWFLs were set up to monitor currents on each respective line via split-core current transformers (CTs).

The pilot showed excellent results, except for the lines that terminated into a transformer. We found that when there were long tap lines, the location calculated by the TWFLs would be the tap's location. This was useful information, but not critical to locating a fault. Since the pilot was successful, we started a program to install TWFLs on our 500 kV system, which had previously yielded poor locations.[1] As a result, we amended our standard construction design to include the installation of TWFLs on new 500 kV lines.

Since the pilot and updating the standard, we have successfully installed TWFLs to achieve coverage of most of our 500 kV network using point-to-point coverage and through-coverage. In the context of our approach, point-to-point coverage would be if TWFLs were installed at Substation A, B, and C. Through-coverage would be if TWFLs were installed at Substation A and C; post-processing is then performed to calculate fault locations on each line. We have proven the accuracy of through-coverage on our system and have used the method to reduce cost and labor associated with installing new devices. Fig. 1 illustrates the concept of point-to-point and through-coverage with TWFLs.

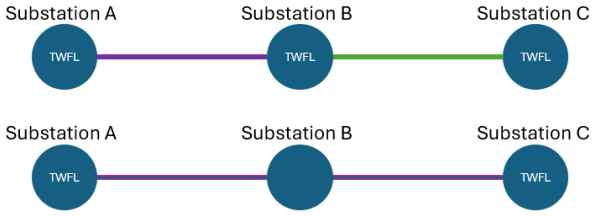

Fig. 1. Through-coverage vs. point-to-point coverage.

[1]We would later conclude that poor locations from traditional fault locating devices were due to static wire flashover during faults. [6].

As our TWFL coverage increased, we expanded our coverage from 500 kV lines to long lines with low characteristic impedance on which we had trouble locating faults. Implementing this selection process led us to one of the questions we sought to answer in this paper: how can we analytically select our TWFL deployment locations and strategies to achieve the maximum gain for the minimum deployment cost?

This question is multilayered. First, using the point-to-point coverage method, we needed to determine the minimum number of TWFLs that needed to be deployed to attain complete coverage of our system. We used graph theory methods to build a mathematical representation of the lines on Dominion's network at each voltage level.

Next, the relative "weight" of each line had to be considered. The weight is a normalized scalar value based on the line's attributes. Many factors were considered when calculating this parameter: the number of historical outages, the number of connected customers, line homogeneity, and line voltage. Using the coverage graph and the weight yielded a solution for the optimum placement of TWFLs that maximized coverage and provided the greatest practical benefit for fault locating.

In our current traveling wave monitoring system, we use products from two different vendors but have noticed inconsistencies in the fault location results provided by each vendor's solution. Both vendors use double-ended fault location, which relies heavily on the accurate timestamping of the first arrival time. To address the inconsistencies, we decided to evaluate the performance of two TWFL products from different vendors.

However, due to the sparse and sporadic nature of transmission line faults, we have limited data available for evaluation. So we conducted a hardware-in-the-loop (HIL) test using a real-time electromagnetic transient power system simulator to compare the performance of the two products. Our approach was to develop a 500 kV transmission line model and simulate faults at various locations, inception angles, fault types, and resistances. Details on the HIL test will be discussed in Section III.

II. Optimal Deployment of TWFLs: Dominion Case

To choose the optimal deployment location for TWFL devices, the model of the power grid needed to be decomposed into a series of nodes (substations) and edges (transmission lines) that formed a graph. The bidirectional flow of power on the network suggested that the model could be represented as an undirected graph, denoted as $G = \{N, E\}$, where N represents the set of nodes and E represents the set of edges. Our optimization problem was to simplify our system by removing all nodes and edges where the nodes have only two edges. In mathematical terms, this problem can be stated as follows:

$$G' = (N', \mathrm{E}') \tag{1}$$

$$G' = G \setminus (\{n \in \mathrm{N} \mid deg(n) = 2\}) \cup$$

$$\{e' \mid e' = (u, w), (u, n) \in E, (n, w) \in E, deg(n) = 2\} \tag{2}$$

Where

$$G' = Contracted\ graph$$

$$N', E' = Contracted\ set\ of\ vertice, and\ edges$$

$$\{n \in \mathrm{N} \mid deg(n) = 2\}$$
$$= Set\ of\ nodes\ with\ a\ degree\ of\ 2\ in\ G$$

$$\{e' \mid e' = (u, w), (u, n) \in E, (n, w) \in E, deg(n) = 2\}$$
$$= New\ edges\ formed\ from\ edges\ with\ degree\ of\ 2$$

A. Assumptions and Approach

To produce a practical solution, we operated under the following assumptions:

1) One TWFL will monitor any number of lines within a substation.
2) All lines at a particular voltage level are in the same control enclosure.
3) A set of TWFLs can monitor an infinite number of lines if there are no nodes between them at the same voltage level with more than two edges.
4) TWFLs will only monitor transmission line currents. No voltage-based traveling wave monitoring will be employed.

Our approach to the TWFL placement algorithm was different than other approaches employed in the industry. Our objective was to create a blueprint, based on the unique configuration of our system, that we could use to determine high-value fault locations so we could prioritize installation. Our goal was not to determine the absolute minimum number of devices needed on the network. Future system topologies or temporary switching conditions could be explored by taking an online approach; while intriguing, this is beyond the paper's scope.

Modern TWFLs can capture traveling waves from a monitored current or voltage. We developed a use-case that monitored voltage on our system to avoid the transformer attenuation effect. However, due to the bandwidth limitation on the coupling-capacitor voltage transformer (CCVT), the voltage signal had to come from the earth ground of the CCVT capacitor stack or from the tap on the transformer bushing [4]. A line outage is required to install a TWFL unit, which was not ideal. Also, on our system, the communication-assisted relay schemes require wave traps, which can block signals in the traveling wave range, adding a further layer of complexity. Thus, we chose to use only current-based monitoring for our use-case. Voltage-based monitoring can be considered at certain locations where current-based monitoring is impractical or impossible, but it was excluded from this study.

B. Strategy Outline

To begin our analysis of the optimal deployment strategy, we obtained a text-file copy of the system model that was exported from the energy management system (EMS). This model file contains line names, associated segment names, and tap substations for every line on the system.

The first step was to collect these segments into a "line group." This allowed us to link a single transmission line with multiple sources to aggregate information about each line and substation. Table I shows an example of the structure of model file and how a line group would be denoted.

TABLE I
EXAMPLE OF HOW LINE SEGMENTS CAN BE COLLAPSED INTO "LINE GROUPS"

Line Name/Group and Terminals	Segment A Station	Segment B Station	Segment Name
Line "1", Clearwater - Sabrepoint	Clearwater	Townfield	A
	Townfield	Walley	B
	Walley	Sabrepoint	C
Line "2", Anchor – Ridgefield	Anchor	Ridgefield	A
Line "3", Graypoint – Riverview	Graypoint	Riverview	A

With each line group, we programmatically determined where the line terminated in a breaker or a radial condition by finding the stations that only occurred once in the line group. In Table I, for example, Clearwater and Sabrepoint each occur once, so our script determined that these were the terminals of Line 1. Using the line group names and terminals, we queried a database for line characteristics like length and voltage level. We used a second database that had information on connected customers, history of outages, and miles of overhead and underground construction.

Once this information had been collected and stored within the line group, a weighting algorithm was applied to calculate the relative "weight" of each line group. The weight for each feature was determined using normalization techniques detailed in Equation (3).

$$X' = \frac{X - min(x)}{max(x) - min\,(x)} \tag{3}$$

Where

$X' = normalized\ value$

$x = original\ value$

Application of Equation 3 resulted in an array of values for each feature with a maximum value of 1. With each feature normalized, priority could be assigned by applying scaling factors. For instance, transmission line "A" may have the most connected customers (5,000) and 3 historic outages in the past two years. Transmission line "B" may have the most historic outages (10) and 1,000 connected customers. If a line's the minimum number of connected customers and historic outages are both 0, line "A" would have a weight of 1 for connected customers and 0.3 for historic outages. Line "B" would have a weight of 0.2 for connected customers and 1 for the historic outages. Therefore, the unscaled weight of line "A" would be 1.3 and "B" would be 1.2. Scaling factors could then be applied as necessary to produce weights that make intuitive sense.

With the weight calculated, the line groups could be separated into distinct groupings based on voltage level. The resulting series of graphs contained edges (lines) that connected nodes (substations) for each voltage level considered. The assessment relied on the assumption that a pair of TWFLs, at two substations, can monitor an unlimited number of lines between if the substations between only have two lines connected at a given voltage level. Applying this principle allowed us to drastically change the shape of the graph by reducing the number of edges and nodes. Fig. 2 shows a sample of a small section of the 115 kV network before and after contraction of the nodes.

Performing the contraction posed a challenge: How to retain the weight of the original edges so that the resultant edge maintains this weight? The solution was to redistribute the weight of the edges every time a node was removed. For example, if a node A was connected to node B which was connected to node C, node B would be a candidate for removal. Edges AB and BC would collapse to form edge AC. When node B was removed, the weights of edges AB and BC would be summed to form the weight of edge AC. When the system was collapsed to the point where there were no more collapsible nodes, the sum of the weights of all edges at each node could be summed to form a cumulative weight. The list of reduced nodes, sorted by weight, became a roadmap for the ideal locations to install TWFLs.

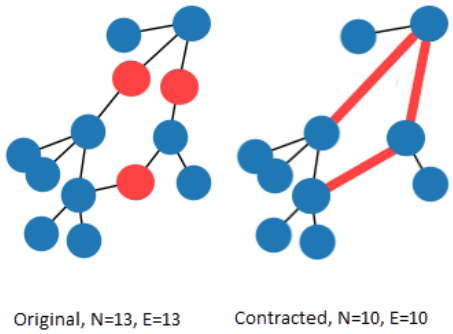

Fig.2. Demonstration of the node contraction technique where nodes marked in red are removed to form edges also marked red.

C. Results and Summary

The results of the study revealed a set of high-impact locations that could guide installation of new TWFLs. We cross-referenced this list with our list of existing TWFLs to reduce the list. While several of the highest-weighted substations already had TWFLs installed, many high-impact installations had not been considered. The report generated listed the results as below in Fig. 3.

STATION 'DRYDEN' has a weight of 0.5932 but already has a TWFL installed

STATION 'MESER' has a weight of 0.43537

TWFL installation gives coverage of:

('MESER', 'DRYDEN')

('MESER', 'CLAYTON')!

('MESER', 'SHUNDER')!

('MESER', 'PLANESTO')

Fig. 3. Output of detector placement algorithm.

When a collapsed line that could be monitored by TWFLs was identified, we checked the remote substation for an existing TWFL. If there was not one, a "!" was added to the terminal substation's name in the report, to identify the line for consideration when prioritizing future installations; at that time, budgetary factors would need to be factored into the weighting algorithm.

The graph reduction yielded a significant reduction in network size, which simplified the process to select TWFL deployments. Table II below shows the original network size for each voltage level and the contracted size.

The table indicates that the 230 kV network showed the greatest reduction in size, indicating that it had many stations with two connections. The 115 kV network also showed the potential for a 38.2% contraction. Across all voltage levels, we saw a total reduction of 331 nodes, which amounts to 53.4% fewer TWFL devices required than without applying contraction methods, to cover the entire network. This reduction demonstrates the value of the graph-based nodal contraction for increasing fault location coverage while reducing installation costs.

TABLE II
UNCONTRACTED VS. CONTRACTED GRAPH NODE AND EDGE COUNT

Voltage Level	Uncontracted		Contracted		% Node Reduction
	N	***E***	***N'***	***E'***	
500 kV	49	60	39	49	20.4
230 kV	358	272	118	162	67.0
138 kV	13	10	9	5	30.8
115 kV	191	196	118	115	38.2
69 kV	14	12	10	7	28.6

In the previous sections we outlined our process for determining TWFL installation locations. We took our network at each voltage level and reduced it to a graph consisting of substation and line groups by eliminating substations that only had two connected lines for a given voltage level. We used weighting and normalization based on factors that were critical to determining restoration difficulty and priority allowed us to develop a priority-based roadmap of TWFL installation locations.

III. HARDWARE-IN-THE-LOOP PERFORMANCE ASSESSMENT USING EMT SIMULATION

In this section, we present the details of the TWFL performance assessment using a real-time electromagnetic transient (EMT) power system simulator. It is important to note that the purpose of this test was not to determine the best technique used by each vendor for timestamping the first arrival time. Rather, it was intended to document our findings. The results obtained from the laboratory setting may not necessarily align with those observed in the field.

A. Hardware-in-the-loop Laboratory Setup

This study evaluated two TWFL products from two vendors, internally known as Product Alpha and Product Bravo. Fig. 4 outlines the hardware-in-the-loop (HIL) laboratory setup. These products monitored the line currents through voltage signals sourced from the simulator and were synchronized by the same GPS clock in our laboratory. Notably, the simulator's analog outputs operated within ± 10 volts, despite representing current signals within the system model. Therefore, before proceeding with the test, we ensured that the tested product could accept the small voltage signal.

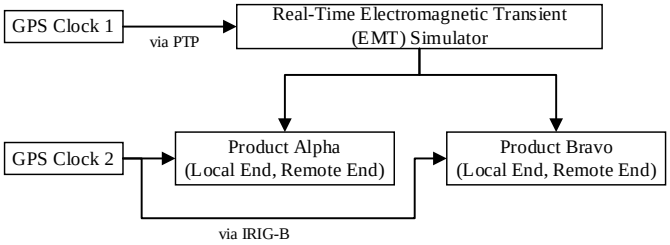

Fig. 4. Hardware block diagram

Both products employ proprietary split-core CTs for line current monitoring. However, the precise operational mechanisms of these CTs were not fully integrated into our testing model, as their details were proprietary. One vendor disclosed that their CT functions as a hybrid CT and high-pass filter. As a workaround, we incorporated a Butterworth filter element into the simulation model with a cutoff frequency set at 2 kHz to effectively eliminate 60 Hz components.

Throughout the testing phase, we encountered challenges where certain fault scenarios did not trigger the TWFL product. Given the thousands of scenarios available, it was difficult to determine which TWFL-generated record corresponded to each scenario run in the EMT simulator. To resolve this problem, we synchronized the simulator to another GPS clock via PTP (Precision Time Protocol). This allowed us to store the precise run time of each scenario for comparison with the data recorded by the TWFLs.

For the split-core CT installation, Product Alpha was connected to the secondary wiring from the protection CT for each phase. However, despite calculating all three phases, it only provided one timestamp based on its internal algorithm.

Product Bravo's split-core CT was also connected to the secondary wiring from the protection CT. like Product Alpha, Product Bravo provides the timestamp for each phase.

B. System Model Setup

In traveling wave fault locating, the energy for accurate detection predominantly resides within the 20 kHz to 2 MHz spectrum [5]. Therefore, it was necessary to employ a frequency-dependent line model, even though it requires significant computation power. The smallest time step that the EMT simulator can provide for this model is 2.8 microseconds. To accommodate this, we had to divide the system model into four cores. Each core took part in the computation in order to get a high-resolution result. Fig 5 illustrates the 500 kV system model and how the cores are arranged.

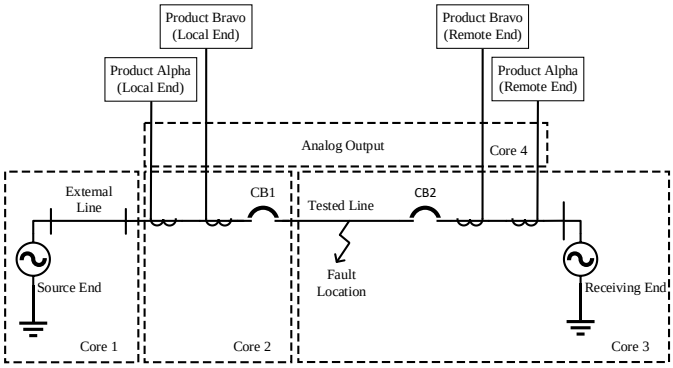

Fig 5. Simplified 500 kV system model.

However, it is important to note the inherent limitation posed by the 2.8 microsecond simulation time step. The minimum line length that the EMT simulator can accurately represent, per the velocity equation using the speed of light, is approximately 0.839 km (0.522 miles). Therefore, if the calculated error is less than 0.839 km, performance within that range cannot be differentiated.

C. Fault Scenarios

To comprehensively evaluate the performance of each product, we conducted extensive testing under various fault conditions, including:

- *Fault types:* AG, AB, ABG, ABC, and external AG.
- *Fault inception angles:* ranging from 0 to 345 degrees at intervals of 15 degrees.
- *Variation in fault resistances:* 0.01 ohms, 0.1 ohms, 1 ohm, and 10 ohms.
- *Fault locations*: spanning 1, 5, 10, 20, 30, 40, 50, and 99% of the line length.

This comprehensive assessment resulted in a total of 3,840 fault scenarios. Each scenario took approximately 30 seconds to compile on the simulator. The total run time for all scenarios was about 32 hours.

D. Assessment Result

Figs. A1, A2, and A3 in Appendix A depict the error distances calculated by TWFLs in each fault scenario. Each 3D scatter chart represents a fault type with a fixed fault resistance. The X-axis displays the fault location, the Y-axis displays the fault inception angle (FIA), and the Z-axis displays the error distance. The magenta cross marker denotes that the TWFLs were either not triggered or the recorded timestep was not able to be paired to provide a valid location from both ends. Both products had their trigger threshold set at 20%.

As shown in Fig. A1, for those scenarios that triggered Product Alpha, the errors are all within 0.1 km. However, when the fault was at 99% of the line, these scenarios had higher errors, with a consistent error of ~1 km. This could have been due to the system configuration with the power source placed at the local end. Additionally, Product Alpha performed poorly for the ABC balanced fault scenarios except when the faults were at 1% and 99% of the line. Moreover, fault resistance did not have an effect on fault locating.

Similar results were obtained for Product Bravo in Figs. A2 and A3, for the A and B phases. We noted that Product Bravo also had a higher error, with a consistent error of ~1 km when the fault was at 99% of the line. Furthermore, in many scenarios Product Bravo had an approximate 7.9 km error (4.9 miles). Like Product Alpha, fault resistance did not have an effect on fault locating.

E. Summary

The purpose of our study was not to discern the technical differences between Products Alpha and Bravo in terms of the traveling wave time stamping algorithm. We just wanted to document the findings using a real-time, EMT power system simulator. The results we observed may not necessarily apply to actual field environments.

Our tests revealed that both Products Alpha and Bravo failed to detect traveling waves when the faulted voltage was close to the zero crossing point, specifically 0, 180, and 345 degrees. This may be due to the fact that the energy of the traveling waves generated around the zero crossing point was not high enough to trigger the TWFLs. We also found that the fault resistance did not impact the traveling wave fault locating capabilities of either product.

Overall, HIL EMT simulation could not differentiate the performance variance between Products Alpha and Bravo, as both products provided similar accuracy and fell within the inherent limitation of 0.839 km (0.522 miles) due to the 2.8 microsecond timestep.

IV. Conclusion

Our detector placement study examined a new deployment strategy for choosing installation locations for TWFLs on the Dominion network. Using applied graph theory and edge-reduction, based on TWFL capabilities, we outlined a method to create a priority-driven list of locations for installations.

On the topic of detector placement strategy, future work may include:

- Combining online algorithms with real-time conditions to optimize TWFLs to calculate fault locations
- Integrating future topologies to better plan for new system arrangements
- Incorporating voltage-based methods into a study
- Incorporating into the weighting algorithm geographic properties like river or mountain crossings

- Exploring adding transmission planning functions to the weighting algorithm

We also conducted a comprehensive assessment of two TWFL products from different vendors using a real-time EMT power system simulator. Our study revealed the limitations of the EMT simulator when evaluating TWFLs. In the next phase, our study will evaluate products from additional vendors and explore interoperability across all products.

Regarding TWFL performance, future work may include:

- Evaluation of traveling wave fault locating and protection applications in HVDC and offshore wind systems.
- Investigating the integration of traveling wave-based products within IEC-61850 substations.

Continuance of this evaluation will result in a more thorough understanding of the limitations and strengths of each product.

V. References

[1] R. Orndorff, "Evaluation of Travelling Wave Fault Locators at Dominion," in 2012 Fault and Disturbance Analysis Conference

[2] C. Galvez and A. Abur, "Fault Location in Power Networks Using a Sparse Set of Digital Fault Recorders," in *IEEE Transactions on Smart Grid*, vol. 13, no. 5, pp. 3468-3480, Sept. 2022

[3] E. C. M. Maritz, J. M. Maritz and M. Salehi, "A Travelling Wave-Based Fault Location Strategy Using the Concepts of Metric Dimension and Vertex Covers in a Graph," in *IEEE Access*, vol. 9, pp. 155815-155825, 2021

[4] D. Cole and M. Diamond, "Implementation of Double Ended Travelling Wave Fault Location When One End is a Transformer Feeder," in 2013 Fault and Disturbance Analysis Conference

[5] E. O. Schweitzer, A. Guzmán, M. V. Mynam, V. Skendzic, B. Kasztenny and S. Marx, "Locating faults by the traveling waves they launch," 2014 67th Annual Conference for Protective Relay Engineers, College Station, TX, USA, 2014, pp. 95-110

[6] R. Orndorff, G. Alvarez, G. Illunga, M. Till, K. Vance, "Segmented Static Wires and Fault Location," in 2023 Fault and Disturbance Analysis Conference

VI. Biographies

Te-Yu Lin joined Dominion Energy as an Engineer II in 2022. His current responsibilities include performing fault analysis and location for transmission systems. He also has three years' experience in designing power distribution systems for semiconductor factories and data centers in Taiwan and the United States. He received his BS in Electrical Engineering from National Taiwan University of Science and Technology in 2016, and his MS in Electric Power Systems Engineering from North Carolina State University in 2020.

Keanan A. Zafar is an Engineer III in the Dominion Energy System Protection Automation and Analysis (SPAA) group. He has 6 years' experience working in Dominion Energy's distribution and transmission control rooms. In 2021, he moved to his current role within SPAA where he works as an electrical engineer and full-stack developer creating operational tools. He holds a bachelor's degree in mechanical engineering and a master's degree in information technology with a software development focus, both from Virginia Tech.

Robert M. Orndorff has been at Dominion Energy since 1984. He spent 11 years as a field relay technician and moved to the Fault Analysis department in 1997, where he still works. His interests include fault location, grid frequency events, and analyzing unusual operations. Robert graduated from J Sargeant Reynolds Community College in 1986 with an AAS degree in Electricity and Electronics. He is a member of IEEE and has been a member of the TRUC planning committee since 2003.

Micah J. Till is the manager of System Protection Engineering at Dominion Energy. His work history includes Dominion Energy's Special Studies, Reliability Engineering, System Protection Engineering, Electric Transmission Planning, and Operations Engineering groups. He has also worked at Tennessee Valley Authority in Chattanooga and ABB Group in Baden, Switzerland. He received his PhD from the University of Tennessee, Knoxville in 2017.

VII. Appendix

FIG. A1

CALCULATED FAULT LOCATION ERROR FOR PRODUCT ALPHA (A-PHASE) FOR SEVERAL DIFFERENT TYPES OF FAULTS AT DISCRETE LOCATIONS

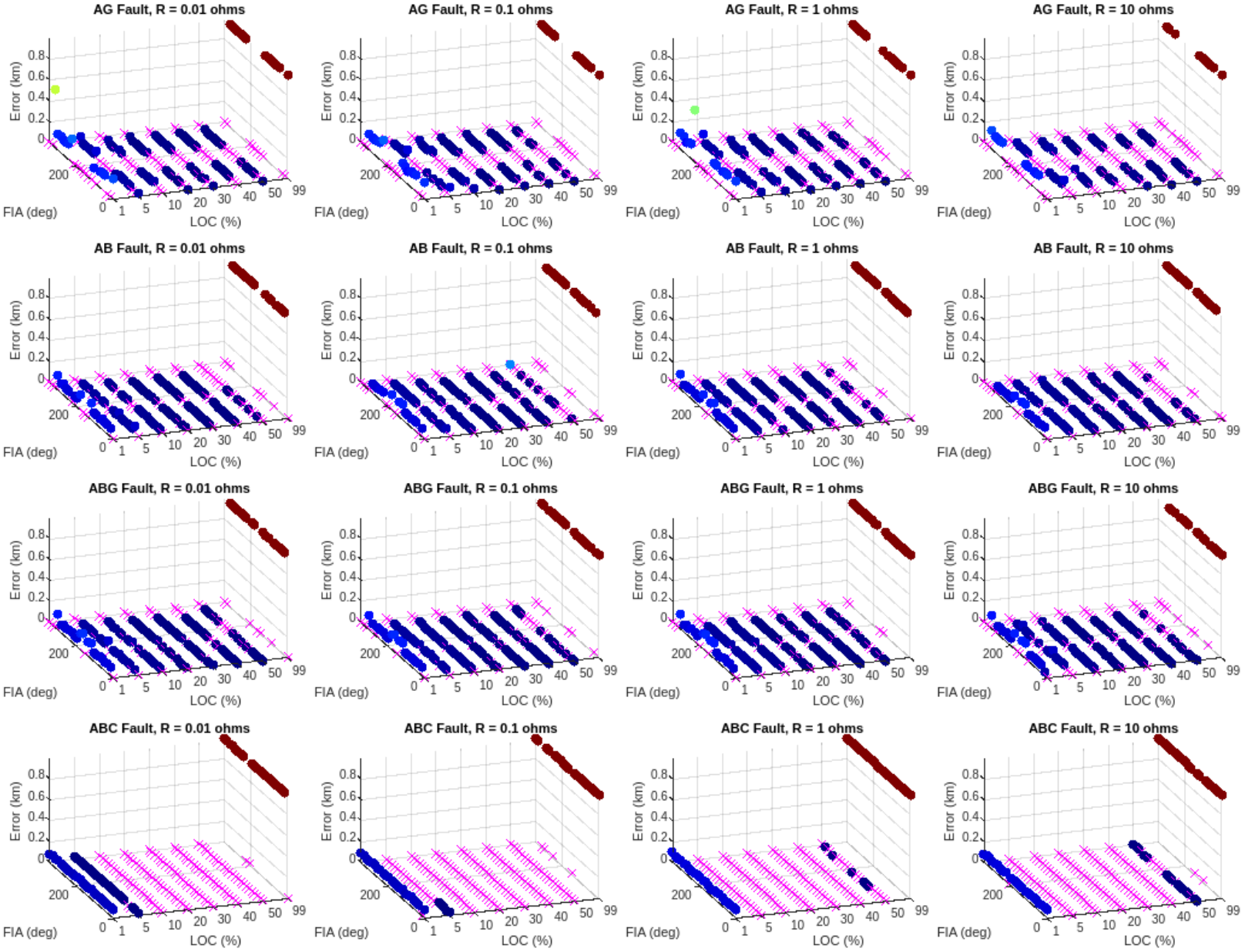

Fig. A1. Varying fault type, fault resistance, and fault inception angle applied to discrete sections of the line produce varying error for Product Alpha.

FIG. A2

CALCULATED FAULT LOCATION ERROR FOR PRODUCT BRAVO (A-PHASE) FOR SEVERAL DIFFERENT TYPES OF FAULTS AT DISCRETE LOCATIONS

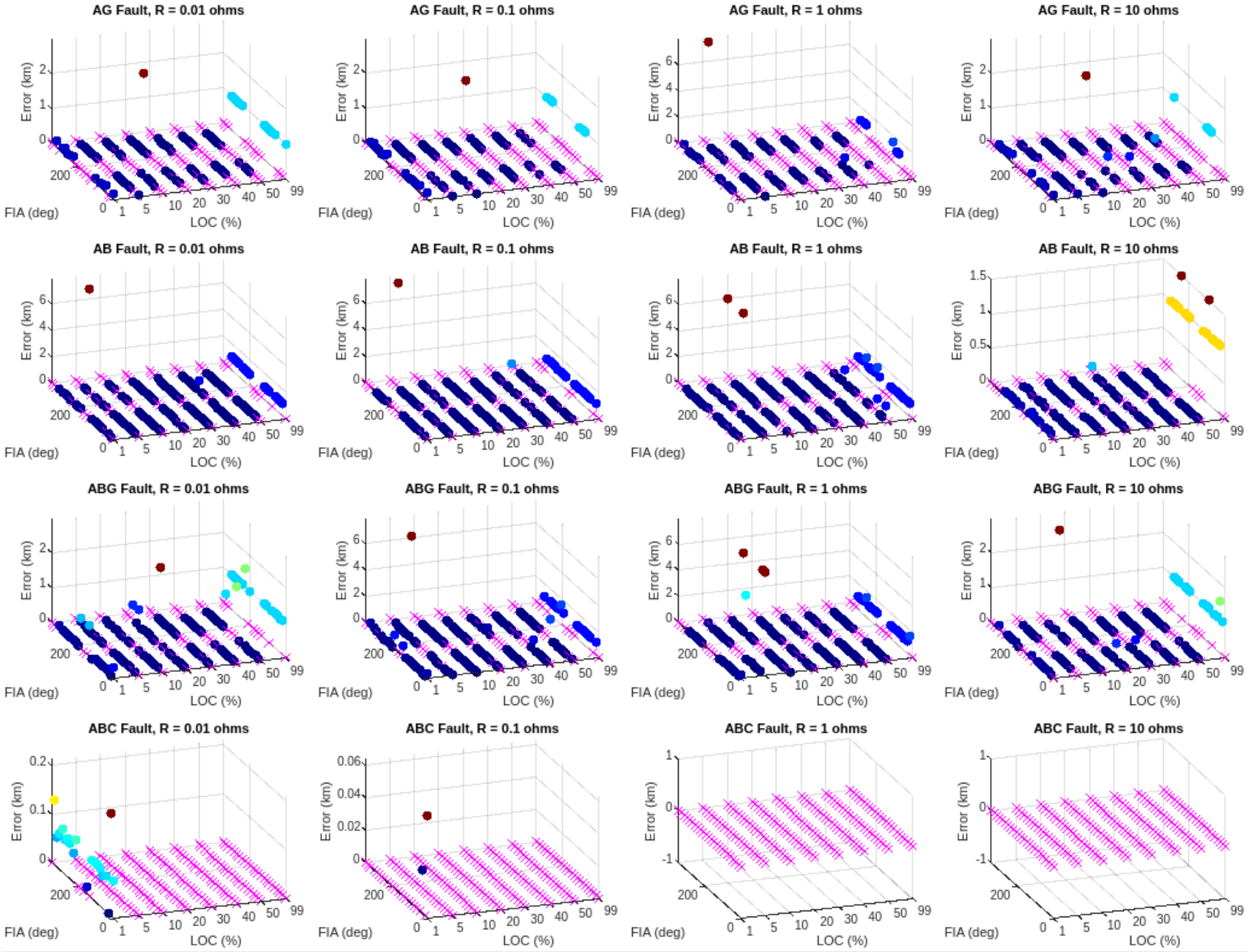

Fig. A2. Varying fault type, fault resistance, and fault inception angle applied to discrete sections of the line produce varying error for Product Bravo when referencing A-phase.

FIG. A3

CALCULATED FAULT LOCATION ERROR FOR PRODUCT BRAVO (B-PHASE) FOR SEVERAL DIFFERENT TYPES OF FAULTS AT DISCRETE LOCATIONS

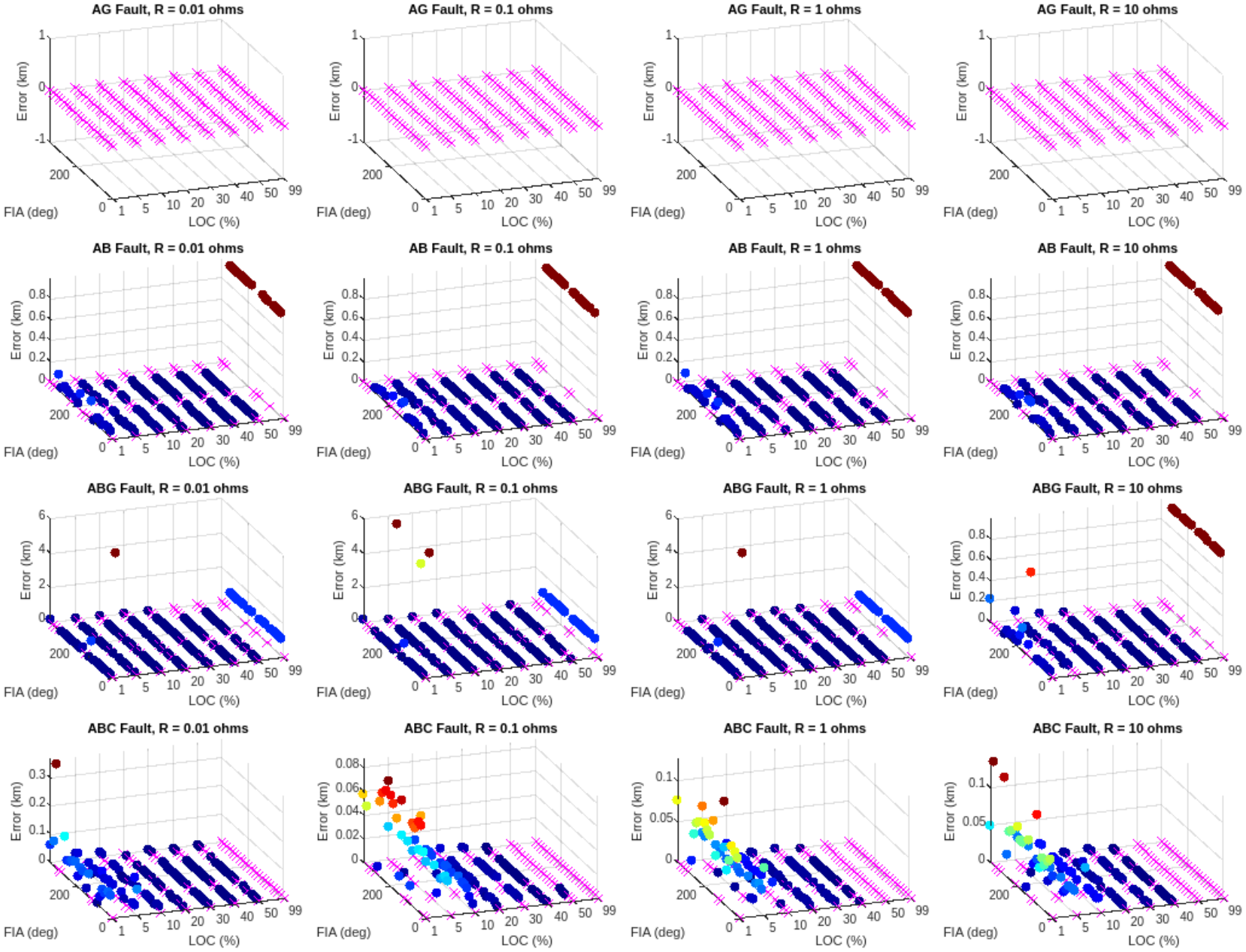

Fig. A3. Varying fault type, fault resistance, and fault inception angle applied to discrete sections of the line produce varying error for Product Bravo when referencing B-Phase.